

## BUDGET OF ANGULAR MOMENTUM AND ENERGY IN TROPICAL CYCLONES

By *E. Palmén*

Academy of Finland<sup>1</sup>

and *Herbert Riehl*

University of Chicago<sup>2</sup>

(Manuscript received 2 September 1956)

### ABSTRACT

The surface stress in tropical storms is computed as a function of the radius, from mean wind data in the troposphere. If only the symmetrical part of the circulation is considered, the stress ranges from 1 dyne per square centimeter in the outskirts to 20 dy/cm<sup>2</sup> at a distance of 1 degree latitude from the center. Inclusion of the mean asymmetry of the wind field, resulting from superposition of steering current and vortex, yields values about 20 per cent higher.

The absolute angular momentum budget shows that most net inward momentum transport is carried by the symmetrical part of the circulation near the core, and that the asymmetrical part contributes up to 50 per cent at a distance of 6 deg lat from the center. Calculation of the angular momentum transport due to the earth's rotation in inflow and outflow layers shows that the vertical momentum transport is directed upward everywhere; outside the 2-deg radius, this transport is accomplished by eddies.

Generation and dissipation of kinetic energy are calculated. The generation depends on the vertical correlation between radial flow component and pressure gradient which, for production of kinetic energy, must be positive, *i.e.*, the strongest inflow must occur at the strongest inward directed pressure gradient. This shows that kinetic energy production within the cyclone can take place only if the cyclone is of the warm core type.

Next, the importance of a local heat source at the ocean surface for production of the observed inward warming in the rain area is discussed, and a relation between the local heat source and the central pressure is given. A general energy balance shows that about 3 per cent of the latent heat released is converted to kinetic energy, and that a considerable export of potential plus internal energy takes place from tropical storms.

### 1. Introduction

The increasing amount of upper-air information available in tropical storms has made possible estimates of heat and momentum balances in these cyclones. As yet, the data are still somewhat uncertain, so that the balances must be regarded as preliminary and subject to later revision. Nevertheless, enough information on the mechanisms of heat and momentum exchange in tropical storms can be gained at the present stage of observational knowledge to justify presentation of the preliminary results.

### 2. Observations

In this article, only average properties of tropical cyclones will be considered. The mean thermal structure of the rain area will be that computed by Schacht (1946); since reliable moisture measurements still do not exist on account of observational difficulties, saturation will be assumed above the sub-cloud layer. Studies of the mean wind distribution have been made by Hughes (1952) at the low-level recon-

naissance flight level (500 to 1000 ft) and by Jordan (1952) at upper levels from 4000 to 45,000 ft. Since balloon runs are eliminated selectively at high surface wind-speeds on account of release difficulties, the two sets of wind data are not quite compatible. For internal consistency, surface values used in this article have been obtained by downward extrapolation of the vertical distribution obtained by Jordan, especially of the tangential wind component, with allowance for surface frictional effects. This procedure underestimates the low-level windfield beyond the smoothing introduced by the averaging process in the original wind calculations, so that the values of all fluxes to be shown will be very conservative. A uniform top of the storm has been assumed at 100 mb, which appears reasonable in view of the fact that near this level most rawins show a rapid turning with height to undisturbed stratospheric easterlies.

The vertical distribution of the tangential component ( $v_\theta$ ) at all levels from 4000 to 45,000 ft between radii of 2 and 6 deg lat from the center follows a law of the form  $v_\theta = a - b \ln r$  (figs. 1 and 2). Inside of the 2-deg radius, no mean winds were computed by Jordan, because of insufficient observations. However, a profile at the 1-deg radius has been extrapolated from the power law.

<sup>1</sup> Participated under contracts between the Office of Naval Research and the University of Chicago while on leave in Chicago.

<sup>2</sup> Participated under contracts between the Office of Naval Research and the University of Chicago.

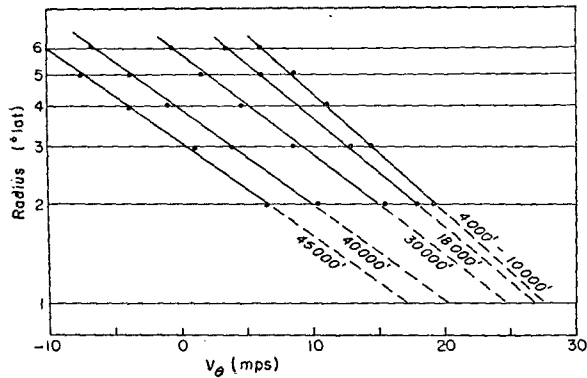


FIG. 1. Profiles of tangential velocity against radius at different elevations.

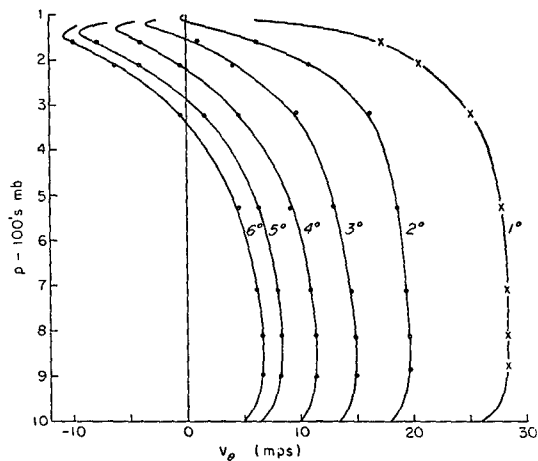


FIG. 2. Profiles of tangential velocity against pressure at different radii.

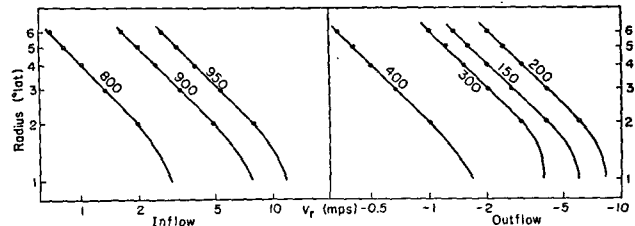


FIG. 3. Profiles of radial velocity against radius at different pressures.

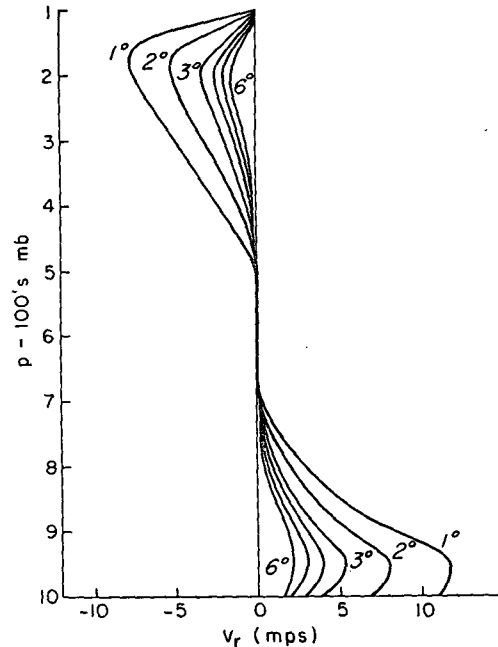


FIG. 4. Profiles of radial velocity against pressure at different radii.

Vertical profiles of the radial component ( $v_r$ ) are difficult to construct, because of uncertainties in the data. Jordan found inflow decreasing upward below 10,000 ft, and intense outflow in the high troposphere, with the peak at 40,000 to 45,000 ft. At intermediate levels, the individual values of  $v_r$ , which were averaged ranged widely from inflow to outflow; in the net, they gave inflow. Because of the wide spread of values, however, they were not considered representative; it was best to state conservatively that inflow occurred in the low troposphere and outflow in the high troposphere, with variable conditions in the middle troposphere.

For the present purposes, vertical profiles of radial velocity are necessary. Three facts are available as guides for the construction of these profiles:

1. The integral of  $v_r$  from the surface to 100 mb must vanish at any radius to satisfy mass continuity, assuming steady state.
2. Outside the 2-deg radius, there is hardly any net convergence at the reconnaissance flight level; in some storm sectors, there is even a small divergence. This agrees with the mean weather distribution, which shows that most ascent takes place quite close to the center.

3. The temperature increases toward the center in the rain area above 10,000 ft and is nearly constant at low levels. If large masses of air with potential wet-bulb temperature characteristic of the environment were brought into the central region in the middle troposphere, the observed temperature structure could not exist. It follows that the inflow must be restricted to the low troposphere.<sup>3</sup>

On the basis of these criteria, the low and high tropospheric parts of Jordan's calculations were retained without modification, but the mid-tropospheric inflow was eliminated. Fig. 3 shows the radial velocity profiles as a function of pressure, fig. 4 as a function of the radius by use of the relation  $v_r r = \text{constant}$  to the 2-deg radius. Again an extra-

<sup>3</sup> It should be noted, however, that in some instances, especially large typhoons, there is a broad outer envelope extending as far as 10 deg lat radius from the center in which a cyclonic circulation with speeds of 25 to 40 kn exists even at 500 to 400 mb. The production of this circulation may be explained if one postulates some inflow in the middle troposphere in the outer envelope. Radial symmetry being assumed, the inflow would take place at nearly constant absolute angular momentum, as it occurs far above the ground-friction layer. Since the distance from the center is large, only small inward displacements are needed to account for the observed tangential speeds. Thus, the upper inflow would not be a part of the primary mass circulation through the storm, with which this article is concerned.

polation to the 1-deg radius has been made, with use of the surface convergence values of Hughes (1952) and the assumption that this convergence decreases upward proportional to the radial speed.

In addition to mean values averaged around rings at given radii from the center, Jordan's study gives values of  $v_r$  and  $v_\theta$  in eight quadrants oriented with respect to the motion of the storm. This permits the calculation of products  $\overline{v_r'v_\theta'}$ , where the primes denote deviations from the mean for a ring, and the bar denotes averaging around the ring. These products give the contribution to the momentum flow due to the mean asymmetry of the windfield which arises from the superposition of vortex and steering current. Although these calculations proved rough and values were highly variable from one level to the next, approximation curves of the products could nevertheless be drawn; they have been utilized in some of the budget computations.

3. Surface stress

We shall consider the equations of motion in cylindrical coordinates  $(\theta, r, z)$  with origin at the center of the hurricane. The radial direction ( $r$ ) is taken positive toward the center, as is the radial component of velocity. In this coordinate system, the horizontal equations of motions are

$$\rho \frac{dv_\theta}{dt} = \rho f v_r + \rho \frac{v_\theta v_r}{r} - \frac{\partial p}{r \partial \theta} + \frac{\partial \tau_{\theta z}}{\partial z}, \tag{1}$$

and

$$\rho \frac{dv_r}{dt} = -\rho f v_\theta - \frac{\rho v_\theta^2}{r} - \frac{\partial p}{\partial r} + \frac{\partial \tau_{rz}}{\partial z}. \tag{2}$$

Here  $\rho$  is the air density,  $p$  the pressure,  $f$  the Coriolis parameter, and  $\tau_{\theta z}$  and  $\tau_{rz}$  are the tangential and radial components of the shearing stresses, respectively. The third equation of motion is the hydrostatic equation, and mass continuity is given by

$$\frac{\partial}{\partial r} (\rho r v_r) + \frac{\partial}{\partial z} (\rho w) = 0, \tag{3}$$

where  $w$  is the vertical component of motion.

We shall consider a radially symmetric cyclone in the steady state. Solving (1) for the shearing stress with these restrictions, and utilizing the mass continuity requirement, we have

$$\frac{\partial \tau_{\theta z}}{\partial z} = \frac{\partial}{\partial r} (\rho v_\theta w) + \frac{\partial}{\partial z} (\rho v_\theta w) - \rho f v_r - \frac{2\rho v_r v_\theta}{r}. \tag{4}$$

A similar transformation of (2) is not necessary, because both the total shearing stress and its radial component can be calculated from the tangential stress and the data of figs. 1 to 4.

The tangential stress must vanish at the upper boundary of the storm. Integrating (4) from the surface pressure ( $p_0$ ) to 100 mb, we obtain the tan-

gential stress as

$$\tau_{\theta 0} = \frac{2}{g r} \int_{p=100}^{p_0} v_\theta v_r dp - \frac{1}{g} \frac{\partial}{\partial r} \int_{p=100}^{p_0} v_\theta v_r dp, \tag{5}$$

where  $g$  is the acceleration of gravity, and use has been made of the conditions that (1) there is no net mass transfer through a cylindrical wall at the distance  $r$  from the center, and that (2) the vertical momentum transport vanishes at top and bottom of the storm.

The tangential stress must be zero, at least approximately, also at the level  $H$  (pressure  $p_H$ ), where  $v_\theta$  reaches a maximum above the friction layer. Integrating (1) from  $p_0$  to  $p_H$  with the preceding assumptions, we have

$$\tau_{\theta 0} = \frac{1}{g} \int_{p_H}^{p_0} \left( f + \frac{v_\theta}{r} - \frac{\partial v_\theta}{\partial r} \right) v_r dp - \frac{1}{g} \int_{p_H}^{p_0} w \frac{\partial v_\theta}{\partial z} dp. \tag{6}$$

As stated earlier, the horizontal divergence, and hence also the vertical motion, are nearly zero outside the 2-deg radius. In this region,

$$\tau_{\theta 0} = \frac{1}{g} \int_{p_H}^{p_0} \zeta_a v_r dp = \frac{p_0 - p_H}{g} \langle v_r \zeta_a \rangle, \tag{7}$$

where  $\zeta_a$  denotes the absolute vorticity about the vertical axis and  $\langle \rangle$  indicates vertical averaging.

Values of  $\tau_{\theta 0}$  are obtained readily from (5) with the data of figs. 1 to 4, because the frictional drag depends only on the vertical wind distribution. Table 1 shows the values of all terms of (5), and interpolated values at radii of 1.5 and 2.5 deg lat from the center.

Equation (7) gives the same surface drag if  $p_0 - p_H$  has the values shown in table 2. According to this table, the level of maximum tangential wind rises from the outskirts of the cyclone toward the interior. On the average, the calculated level agrees well with that found in previous trade-wind studies. According

TABLE 1. Values for all terms of (5).

	Radius (deg lat)							
	1	1.5	2	2.5	3	4	5	6
$2 \frac{v_\theta v_r}{r}$ ( $10^{-4}$ ):	3.14	1.58	0.99	0.70	0.51	0.32	0.21	0.14
$\frac{\partial}{\partial r} (v_\theta v_r)$ ( $10^{-4}$ ):	1.10	0.52	0.33	0.24	0.18	0.13	0.11	0.08
$\tau_{\theta 0}$ ( $dy/cm^2$ ):	18.8	9.8	6.1	4.2	3.0	1.8	0.9	0.6

TABLE 2. Pressure difference between top and bottom of ground-friction layer.

Radius (deg lat):	2	3	4	5	6
$p_0 - p_H$ (mb):	116	106	98	67	54

to Riehl *et al* (1951), the level is situated near 910 mb in the east Pacific trades. Sheppard and Omar (1952) found somewhat lower values, 300 to 800 m, depending on wind speed; higher levels corresponded to higher speeds.

It is of interest to compare the values of  $\tau_{\theta 0}$  in table 1 with those calculated from the well-known empirical formula,

$$\tau_{\theta 0} = k\rho_0 V_0 v_{\theta 0}, \tag{8}$$

where  $k$  is the drag coefficient,  $\rho_0$  the density on the ground, and  $V_0$  and  $v_{\theta 0}$  are total and tangential wind speed at anemometer level, respectively. These latter speeds are not known, only the mean wind for the layer from 1000 to 900 mb. Use of this wind leads to an overestimate of the stress and underestimate of  $k$ . This must be borne in mind when considering table 3. These values are generally lower than those in the trade-wind belt, where  $1.6 \times 10^{-3}$  can be expected according to Sheppard and Omar (1952). In strong winds in the Baltic Sea, Ekman (1905), and Palmén and Laurila (1938), have computed drag coefficients of  $2.4 \times 10^{-3}$ . As just stated, however, the values of  $k$  in table 3 are likely to be too low. If the mean wind components at the 1-deg radius are reduced by as little as 10 per cent, the value of  $k$  at that radius would be  $2.6 \times 10^{-3}$  instead of  $2.1 \times 10^{-3}$ ; similar results are obtained for the other radii. We therefore see that  $k$  as computed from (5) agrees reasonably well with other estimates.

The total surface stress is  $\tau_0 = \tau_{\theta 0} \sec \alpha$ , where  $\alpha$  is the indraft angle. It can be computed by forming the ratio  $v_r/v_{\theta}$ . Table 4 shows calculated values for  $\alpha$  and  $\tau_0$ . The mean indraft angle is remarkably constant; it agrees well with values found by Hughes (1952). Probably, however, the angles are somewhat smaller than would have been obtained from surface wind-measurements, so that the actual surface stress should be somewhat larger than given in the table.

Further comments on the stress calculations, especially regarding asymmetries of the wind distribution, will be made in subsequent sections. The asymmetries have not been included in the foregoing, because they are considered to be the weakest link of the observational material.

TABLE 3. Drag coefficient  $k$  computed from (8).

Radius (deg lat):	1	1.5	2	2.5	3	4	5	6
$k$ ( $10^3$ ):	2.1	1.5	1.4	1.4	1.3	1.1	1.1	1.4

TABLE 4. Indraft angle and total surface stress.

Radius (deg lat):	1	1.5	2	2.5	3	4	5	6
$\alpha$ (deg):	21	20	19	18	17	16	17	20
$\tau_0$ (dy/cm <sup>2</sup> ):	20.1	10.4	6.5	4.4	3.1	1.9	0.9	0.6

#### 4. Angular momentum budget

Some aspects of the mechanisms operating to maintain tropical cyclones are brought out by a computation of the flow of angular momentum across concentric cylinders. The absolute angular momentum  $M = v_{\theta}r + \frac{1}{2}fr^2$ , when expressed in a cylindrical coordinate system with origin at the hurricane center. The flow across a cylinder at a distance  $r$ , between the pressure surfaces  $p_1$  and  $p_2$ , is given by

$$[M]_r = \frac{1}{g} \int_{p_2}^{p_1} \int_0^{2\pi} \left( v_{\theta}r + \frac{fr^2}{2} \right) v_r d\theta dp. \tag{9}$$

In carrying out the integration with respect to  $\theta$ , axial symmetry will be no longer assumed, so that

$$[M]_r = \frac{2\pi r^2}{g} \left[ \int_{p_2}^{p_1} \bar{v}_{\theta} \bar{v}_r dp + \int_{p_2}^{p_1} \overline{v_{\theta}' v_r'} dp + \frac{fr}{2} \int_{p_2}^{p_1} \bar{v}_r dp \right]. \tag{10}$$

Similarly, the vertical momentum flow between the radii  $r_1$  and  $r_2$  is given by

$$[M]_z = 2\pi \left[ \int_{r_1}^{r_2} \rho \bar{v}_{\theta} \bar{w} r^2 dr + \int_{r_1}^{r_2} \rho \overline{v_{\theta}' w'} r^2 dr + \frac{f}{2} \int_{r_1}^{r_2} \rho \bar{w} r^3 dr \right]. \tag{11}$$

The first terms on the right-hand sides of (10) and (11) give the angular momentum transport arising from the axially symmetric part of the wind field, and the second terms that due to the eddy fluxes arising from asymmetries around the radius, especially superposition of vortex and steering current. The third terms measure the flow due to the earth's rotation. In (11), the second integral can also be expressed as a stress term where the stress  $\tau_{\theta z}$  measures the total effect of the whole spectrum of disturbances producing vertical momentum flow. We then have

$$\int_{r_1}^{r_2} \rho \overline{v_{\theta}' w'} r^2 dr = - \int_{r_1}^{r_2} \overline{\tau_{\theta z}} r^2 dr, \tag{12}$$

and the torque exerted by the cyclone on the ground is

$$[M]_0 = 2\pi \int_{r_1}^{r_2} \overline{\tau_{\theta 0}} r^2 dr. \tag{13}$$

We can compute  $[M]_0$  from (10) and (13), because the net convergence of momentum between two cylinders extending from bottom to top of the storm must equal the transport to the ocean for a steady state. For this computation, the first and third integrals of (11) vanish, because the vertical motion is zero at the ground and at the top of the storm; the third integral of (10) is also zero, since no net mass

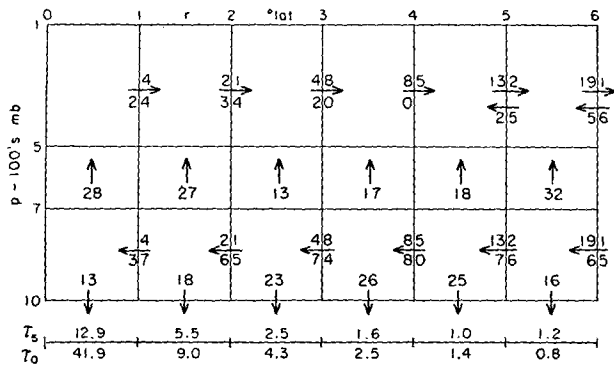


FIG. 5. Angular momentum budget assuming axial symmetry ( $10^{22}$  g  $\text{cm}^2 \text{sec}^{-2}$ ). Horizontal arrows denote flow across radii; upper arrow gives transport due to earth's rotation, lower arrow that due to mean windfield. Downward arrows at bottom show momentum transport to sea, and momentum arrows between 700 and 500 mb show upward momentum transport through this layer. Stress  $\tau_{\theta z}$  is given at 500 mb ( $\tau_5$ ) and at surface ( $\tau_0$ ) below momentum-transport diagram.

flow takes place through any cylinder. Thus,

$$\int_{r_1}^{r_2} \bar{\tau}_{\theta\theta} r^2 dr = \frac{r_2^2}{g} \int_{p=100}^{p_0} (\bar{v}_\theta \bar{v}_r + \overline{v_\theta' v_r'})_{r_2} dp - \frac{r_1^2}{g} \int_{p=100}^{p_0} (\bar{v}_\theta \bar{v}_r + \overline{v_\theta' v_r'})_{r_1} dp. \quad (14)$$

In (10) to (14), only the terms depending on  $\overline{v_\theta' w'}$  cannot be estimated and must be left as dependent residual. As stated earlier, the contribution of the  $\overline{v_\theta' v_\theta'}$  term can be calculated to the extent that the mean asymmetry gives the eddy fluxes and within the limits of reliability of calculating this delicate correlation term.

Figs. 5 and 6 depict the angular momentum budget. Along the vertical, three layers are shown in fig. 5: (1) the low-level layer of inflow, (2) the intermediate layer without pronounced radial flow, and (3) the layer of high-tropospheric outflow. Along the radial direction, the vertical and horizontal transports have been computed at intervals of 1 deg lat. Inside the 1-deg radius, the surface torque has been calculated from continuity. Fig. 5 shows the budget without the

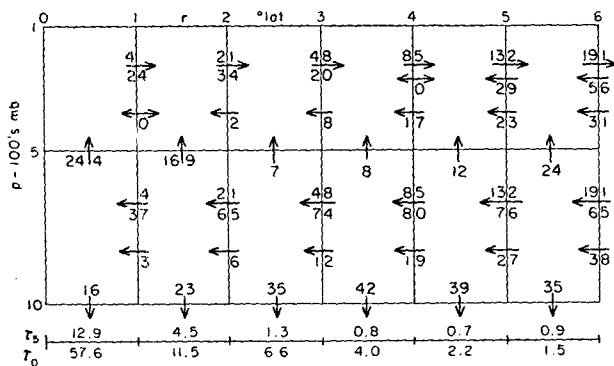


FIG. 6. Angular momentum budget including mean asymmetry. Eddy transport is given by lowest horizontal arrow in each layer. Other notations as in fig. 5.

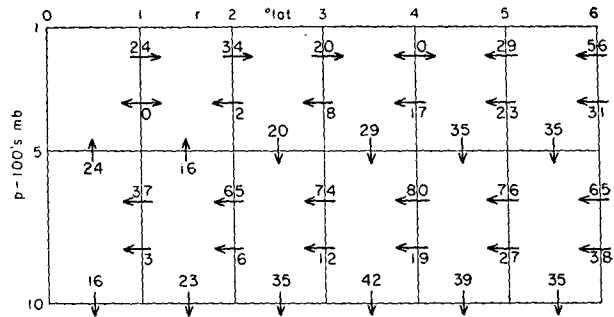


FIG. 7. Angular momentum budget including eddy transport but omitting terms due to earth's rotation.

radial asymmetries; in fig. 6, these asymmetries have been included.

All arrows point in the direction of positive momentum transport. In each layer, the number above the horizontal arrows gives the momentum flow due to the earth's rotation, the number below the arrows that due to the symmetrical part of the windfield. The lowest set of arrows in fig. 6 represents the eddy flow. Outside the 2-deg radius, the vertical arrows denote the eddy transports required to maintain momentum continuity. Between the center and the 2-deg radius, there is also upward momentum flow arising from the general mass-convergence field. This contribution is shown to the left of the vertical arrows. It is seen that, close to the center, most momentum is carried upward by this mechanism; further, the residual vertical eddy flow is smallest when the horizontal eddy flow is included.

A similar computation of the angular momentum budget from the same data has recently been made by Pfeffer (1956). He disregarded the terms containing the Coriolis parameter, since these terms do not contribute to the net momentum transport across cylinders. The eddy fluxes in the free atmosphere, however, cannot be computed in this way. This is illustrated by fig. 7, which contains the same horizontal transport data as fig. 5 but omits the Coriolis terms. We now find a strong eddy transport that is directed downward, against the angular momentum gradient. This transport would correspond to eddy stresses of no less than 3 to 4 dy/cm<sup>2</sup> in the free atmosphere between the 2- and 4-deg radii.

The total surface torque inside a given radius must equal the net inflow of angular momentum across the radius. Thus, one cannot define an outer limit for a cyclone in the symmetric case, because the radial component of motion vanishes by definition at the outer boundary, hence also the momentum transport. The possibility of eddy transport at a boundary remains open. Fig. 6 shows that the eddy momentum-flow reaches 50 per cent of the flow due to the symmetric circulation at the 6-deg radius, as also noted by Pfeffer (1956). The synoptic pattern in many hurricane situations, however, suggests that

TABLE 5. Tangential component of surface stress including asymmetry of momentum transport.

Radius (deg lat):	1	1.5	2	2.5	3	4	5	6
$\tau_{\theta_0}$ (dy/cm <sup>2</sup> ):	24.2	12.3	8.5	6.3	4.8	3.1	1.8	1.3

the symmetric mechanism is the most important one even at large distances from the center. For instance, the requisite momentum inflow can be obtained at the radius where the surface tangential velocity becomes zero if the upper anticyclonic circulation covers a larger area than the surface cyclonic circulation, and this is precisely what happens. Assume that the surface tangential velocity is zero at a distance of 1000 km from the center, that the inward momentum transport is  $2 \times 10^{24}$  g cm<sup>2</sup> sec<sup>-2</sup> at this radius, and that  $v_r$  is given by extension of the non-divergent profiles of fig. 3. The momentum will then be transported by the symmetric circulation alone, according to (10), if the anticyclonic tangential velocity in the upper troposphere is 10 m/sec. Such values are regularly reached or exceeded.

Equation (5) can be used to calculate the surface stress including the asymmetry, if means and deviations of the products  $v_r, v_{\theta}$  are entered into the integrals on the right-hand side. Table 5 shows the values of surface stress obtained by this procedure.

The surface stress is considerably stronger than in the case of symmetry. Values for total stress and the coefficient  $k$  in (8) will increase correspondingly if calculated from table 5. Using the values for the angle given in table 4, one obtains the radial distribution of total surface stress shown in fig. 8. The distribution follows a law of the form  $\tau_0 r^x = \text{const}$ . In the central part of hurricanes, the surface frictional stress may reach very high values. From the power law,  $\tau_0 = 100$  dy/cm<sup>2</sup> at  $r = 0.4$  deg lat, quite close to the average eye boundary. If a wind of 50 m/sec is assumed at this radius, the coefficient  $k = 3.3 \times 10^{-3}$ .

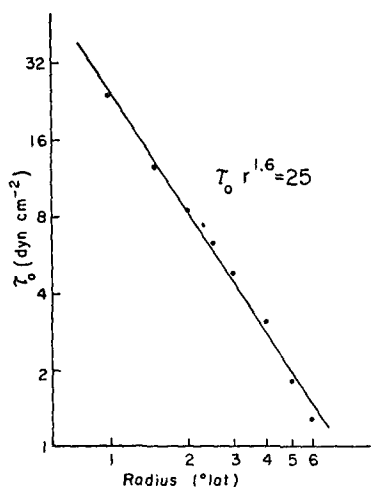


FIG. 8. Distribution of surface stress with radius.

5. Release and dissipation of kinetic energy

Palmén and Jordan (1955) have made previous estimates of release and dissipation of kinetic energy ( $K$ ) from the mean hurricane data of figs. 1 to 4. According to these data, the inflow of kinetic energy across the 6-deg radius is very small, so that the total production of kinetic energy inside this radius must balance the frictional dissipation.

Let  $V$  denote volume and  $S$  the surface of the cylinder at any radius. Then, relative to the moving cyclone,

$$-\int_S v_r K_r dS = -\int_V v_r \frac{\partial p}{\partial r} dV + \int_V \left( v_{\theta} \frac{\partial \tau_{\theta z}}{\partial z} + v_r \frac{\partial \tau_{rz}}{\partial z} \right) dV, \quad (15)$$

where  $K_r$  is the kinetic energy per unit volume at radius  $r$ . The first term gives the inward transport of kinetic energy across the boundary, the second integral represents the work done by horizontal pressure forces inside the volume, and the extreme right-hand integral measures the dissipation due to frictional stresses.

Given the mean radial pressure and wind distribution, the axially symmetric part of the work term is readily computed. Integrating this term between the radii  $r_1$  and  $r_2$ , and utilizing mean values between these radii, we have

$$\int_V v_r \frac{\partial p}{\partial r} dV = \pi(r_2^2 - r_1^2) \int_{p=100}^{p_0} v_r \frac{\partial z_p}{\partial r} dp, \quad (16)$$

where  $z_p$  denotes the height of an isobaric surface. Because this term enters with a negative sign in (15), it will contribute to generation of kinetic energy if  $v_r$  and  $\partial z_p / \partial r$  are negatively correlated along the vertical, *i.e.*, when the low-level inflow occurs at a larger inward directed pressure gradient than the upper outflow. Thus, *kinetic energy is produced only when temperatures increase toward the cyclone center*. The core must be warmer than the surroundings to maintain the cyclone against frictional dissipation. The high core temperatures outside the eye are maintained mostly by release of latent heat of condensation in the air stream rising from the surface. Therefore, it is one necessary condition for formation and maintenance of hurricanes that the potential wet-bulb temperature of the surface current must be so high that, during ascent, this current will become warmer than the surroundings through the troposphere.

Palmén and Jordan (1955) have calculated values of the generation term. From figs. 1 to 4, the transport term of (15) is also obtained. Estimates of frictional dissipation can be made after transformations of the type

$$v_{\theta} \frac{\partial \tau_{\theta z}}{\partial z} = \frac{\partial}{\partial z} (v_{\theta} \tau_{\theta z}) - \tau_{\theta z} \frac{\partial v_{\theta}}{\partial z}.$$

After integration over the depth of the storm, the first of these terms gives the dissipation at upper and lower boundaries, the second the internal dissipation within the troposphere. The dissipation at the top is presumably negligible; very little is known about the internal dissipation. Therefore, only the ground-dissipation term can be calculated. Assuming that this term is the dominating one, we have

$$\int_V \left( v_\theta \frac{\partial \tau_{\theta z}}{\partial z} + v_r \frac{\partial \tau_{rz}}{\partial z} \right) dV = \pi (r_1^2 - r_2^2) (\overline{\tau_{\theta z} v_\theta} + \overline{\tau_{rz} v_r})_0, \quad (17)$$

where the bars indicate mean values over the whole area. These terms can be calculated from the stress values obtained earlier in this article, or as residual in (15). Both methods will be used. Table 6 shows the results of evaluating (15).

Dissipation exceeds generation in the central parts, while outside the 2-deg radius the reverse is true. In a sense, therefore, the high kinetic energy of the central region, the rain area, is maintained by an inflow of kinetic energy from the outer rings. One should not overlook, however, the fact that the energy-generating pressure gradient in the outer rings is produced by high-level outflow of warm air from the rain area.

An estimate of dissipation due to ground friction from (17), with the data of figs. 1 to 4 and table 5, will necessarily be rough, especially in the inner region. Thus, only an order of magnitude comparison with table 6 should be attempted. Table 7 gives the results. Within the limits of accuracy mentioned, agreement between tables 6 and 7 is satisfactory; this strengthens the confidence in the validity of all calculations in this article.<sup>4</sup>

According to Palmén and Jordan (1955), the total kinetic energy of the mean tropical cyclone approximately equals total generation or dissipation in one day. Evidently, a cyclone will decay rapidly if it

TABLE 6. Generation, convergence and dissipation of kinetic energy ( $10^{18}$  ergs/sec) in three rings.

Ring (deg lat):	0.25-2	2-4	4-6	0.25-6
Generation:	48	58	44	150
Convergence:	37	-8	-29	0
Dissipation:	-85	-50	-15	-150

TABLE 7. Dissipation of kinetic energy ( $10^{18}$  ergs/sec) computed from figs. 1 to 4 and tables 4 and 5.

Ring (deg lat):	0.25-2	2-4	4-6	0.25-6
Dissipation:	-87	-30	-11	-128

<sup>4</sup> The dissipation in the free atmosphere should be added to these figures; one can assume that its relative contribution increases outward.

encounters thermally unfavorable conditions. The generation term in (15) will then decrease rapidly; it will become negative if the air ascending in the core is cooler than the surroundings in spite of release of latent heat. This would happen when a storm moves over a relatively cold ocean surface, over a continent, or when colder air masses invade the cyclone near the surface.

## 6. Energy transformations

*Local heat source.*—We have seen that production of kinetic energy depends on a negative correlation between  $v_r$  and  $\partial z_p / \partial r$ , and that such a correlation will occur when the cyclone core is warmer than the surroundings. Confining the analysis to the rain area, we know two principal mechanisms that can produce inward warming: (1) In the average tropical atmosphere, the potential wet-bulb temperature decreases with height to about 400 mb; therefore, if only air from the sub-cloud layer penetrates upward in the core, a warm central region will be created; this consideration was part of the reason for rejecting net inflow in the middle troposphere at the beginning of this article; (2) As shown by Riehl (1954), the foregoing warming mechanism can account for a drop of surface pressure only to about 1000 mb; much warmer temperatures occur in the middle and upper troposphere in the rain area than can be explained by moist adiabatic ascent of air with properties of the sub-cloud layer entering the periphery of the cyclone; a local surface heat-source within the circulation must be assumed to explain the observed thermal structure. Byers (1944) first drew attention to such a heat source on the basis of surface observations. In the outskirts of the cyclone, the temperature drops inward 1 to 2C to the 995- or 1000-mb isobar, indicating adiabatic cooling. Farther inside, the temperature remains constant and the specific humidity increases, suggesting rapid heat transfer from the agitated ocean surface to the atmosphere. The heat so gained by the air is only a minute fraction of that carried inward through the cylinder at the distance of the 1000-mb isobar. Only when the central pressure is as low as 900 mb will the latent heat increase approach 10 per cent and the sensible heat increase 3 per cent. Nevertheless, it is these small increments that produce the strong inward warming and therefore determine the magnitude of the negative correlation  $v_r \partial z_p / \partial r$ . They are thus of utmost importance for generation and maintenance of tropical storms, even though they may be wholly neglected in a general energy balance. This situation is frequently encountered in meteorology, for instance in the general problem of heat exchange between sea and air (Riehl, 1954, p. 374). A small role in a balance sheet does not imply a small role in the mechanism which produces the balance. Kleinschmidt (1951) has

also stressed the importance of the local moisture source. However, he goes so far as to minimize the role of moisture brought into the system from the outside compared to that absorbed from the ocean surface within the storm on a closed path. As the following will show, this position cannot be maintained.

The surface observations can be used for a specification of central pressure in terms of the heat source. We may write the first law of thermodynamics as

$$dh = c_p dT - p^{-1} dp, \tag{18}$$

where  $dh$  is the heat added per unit mass. Along the surface  $dT = 0$ ,  $dh$  must be interpreted to denote a sensible heat increment, since no condensation is taking place. After introduction of the equation of state and the relation  $dh = c_p(T/\theta) d\theta$ , where  $\theta$  is the potential temperature, we find that

$$p_c = p_r(T/\theta_c)^{c_p/R}. \tag{19}$$

Here the integration has been performed between the center ( $c$ ) and the radius where the surface pressure  $p_r = 1000$  mb. It is not possible to extend this approach, because  $\theta_c$  is not independent of the inward pressure drop and the stirring of the ocean water due to the winds generated by the pressure gradient. The purpose in showing (19) is to demonstrate that the central pressure is determined by energy-exchange processes at the surface as well as by the mean temperature of the troposphere above the surface. As pointed out by Haurwitz (1935) and others, it is necessary to postulate an eye with descending motion in order to obtain central temperatures warm enough to permit the cyclone to vanish in the pressure field at the top of the troposphere or, integrating downward from the undisturbed stratosphere, to permit the surface pressure to attain the observed values. We now have a second condition for the occurrence of the observed pressure, namely that sufficient sensible heat energy must be transferred from the ocean to the inflow along the surface to produce values of  $\theta_c$  prescribed by (19), and in turn the upper-air temperature distribution in the rain area leading to the requisite  $v_r \partial z_p / \partial r$  correlation. Only when descent above the center and heat absorption from the ocean occur simultaneously, in the proper relative amounts, can tropical storms be generated and maintained.

*General energy balance.*—If the first law is differentiated with respect to time, and the work term expanded under the assumption of steady state,

$$\frac{dh}{dt} = c_p \frac{dT}{dt} - \frac{v_r}{\rho} \frac{\partial p}{\partial r} + gw. \tag{20}$$

As just discussed, enthalpy changes are zero at the ground; since the vertical motion is also zero, (20) gives a direct relation between production of kinetic energy and the sensible heat transferred from the

ocean. If we now wish to investigate the heat transport through cylinders extending to the top of the storm, the relative importance of the terms in (20) becomes quite different. The absorption of heat from the ocean is so small a fraction of the latent heat released in the ascent that it amounts to no more than the error in estimating the condensation heating, and hence may be dropped. Further, kinetic energy changes are one to two orders of magnitude less than potential energy and enthalpy changes; they can also be neglected as second-order effects. In view of this situation, the information to be gained from (20) is quite limited. It can be used mainly to ascertain the magnitude of the energy transactions and to estimate the efficiency of the cyclone engine in maintaining the circulation.

If the heat gained by the air parcels in passing through the system is given within computational accuracy by the latent heat release,  $dh = -L dq$ , where  $L$  is the latent heat of condensation and  $q$  the specific humidity. In this formulation, the heat sink, radiation, has been omitted in addition to the heat transfer from the ocean. Inserting in (20), we obtain

$$-L \frac{dq}{dt} = \frac{d}{dt} (\Phi + c_p T), \tag{21}$$

and, integrating along a path AB as shown in fig. 9, we have for the large-scale mass flow

$$Lq + c_p T + \Phi = \text{const}, \tag{22}$$

where  $\Phi$  is the geopotential. From Schacht's (1946) hurricane sounding, we can check approximately the validity of (22). In fig. 10, curve b has nearly identical values in the low and high troposphere, in the inflow and outflow layers. Hence, the preceding reasoning can be considered valid within the data limitations.

The quantity  $c_p T + \Phi$  (curve a of fig. 10) increases by about 15 cal/g from the surface to the high troposphere. This increase takes place almost wholly within the 2-deg radius. If the temperature drop due to radiation is 1 C/day, a high value, the heat loss is 0.25 cal/day. Since the air remains within 2 deg lat of the center only for a day or less, it follows that we were justified in omitting radiation from the calcula-

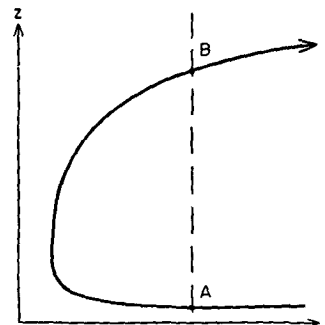


FIG. 9. Path for integration of (20).



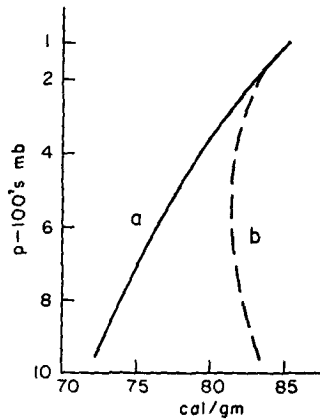


FIG. 10. Vertical distribution of  $\Phi + c_p T$  (curve a) and of  $Lq + \Phi + c_p T$  (curve b) computed from Schacht's (1946) mean hurricane sounding assuming saturation.

tion of  $dh/dt$  along the inner part of the trajectory.

At a cooling rate of 1 C/day, the outflow will reach the surface again after 60 days. In contrast, the average cyclone exists only for six days, fully an order of magnitude less. If one should be able to treat hurricanes as closed steady-state systems, it would be necessary to show that a cold source of sufficient magnitude exists in the storms' surroundings to permit abstraction of all heat gained in the core. We shall consider the situation near the 3-km level, the top of the inflow layer, where the horizontal temperature gradient is still nearly zero. In case of a steady temperature field,  $dT/dt = w \partial T/\partial z$ . After insertion in the first law, we find that  $w = -250$  m/day if the lapse rate is 0.6 C/100 m and the radiation cooling 1 C/day. Mass continuity demands that the inflow through the 2-deg radius, inside which the ascent begins, must equal the downward mass transport through the 3-km surface in the surroundings. Thus,

$$\int_A \rho w dA = \int_0^{2\pi} \int_0^{3 \text{ km}} \rho v_r r d\theta dz, \quad (23)$$

where  $A$  is the area of descent. Utilizing the values of figs. 3 and 4, we find that the diameter of the area of descent is nearly 30 deg lat, considerably larger than the area covered even by the Pacific typhoons. It follows that no cold source of sufficient magnitude exists in hurricanes that would permit application of the closed circulation concept. It is only by means of removal of heat through the outflow to other members of the general circulation that the hurricane can be maintained.

A moisture calculation corroborates this conclusion. For a closed system in steady state the moisture loss due to precipitation must be balanced by evaporation over the area of the closed system. The daily precipitation inside the 2-deg radius is  $2 \times 10^{10}$  tons from table 8. If this is assumed to be the total precipitation, and if the diameter of the closed area is 30 deg

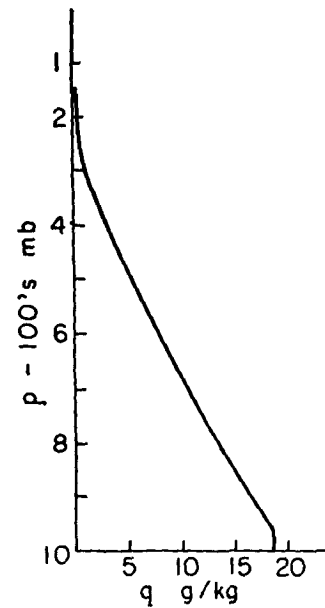


FIG. 11. Distribution of specific humidity with pressure assuming saturation in Schacht's (1946) mean hurricane sounding.

lat, the mean evaporation rate over the area is 0.3 cm/day, a reasonable value. If, however, a more realistic value is assigned to the hurricane diameter, say 15 deg lat, the mean evaporation rate becomes more than 1.0 cm/day which is much too large. It follows that both from heat and moisture balance considerations the hurricane must be regarded as an open system.

If we take the volume integral of (21) and transform to the surface integral over a cylinder with radius  $r$ , extending from the ground to 100 mb,

$$\begin{aligned} \frac{L}{g} \int_0^{2\pi} \int_{p=100}^{p_0} q v_r dp r d\theta \\ = -\frac{1}{g} \int_0^{2\pi} \int_{p=100}^{p_0} (c_p T + \Phi) v_r dp r d\theta. \end{aligned} \quad (24)$$

We shall now take  $r = 2$  deg lat and evaluate the symmetrical part of the heat transport from figs. 3, 4 and 10, and the moisture flow from fig. 11. The

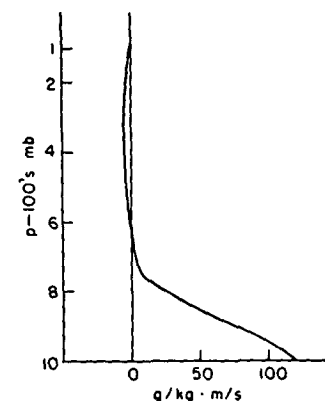


FIG. 12. Product  $qv_r$  as function of pressure.

TABLE 8. Values of all terms in (22), (10<sup>12</sup> kilowatt-hours per day).

Term	Value	
Inflow of latent heat:	13.3	
Inflow of enthalpy:	22.8	
Outflow of potential energy:		36.4
Balance:	36.1	36.4

product  $qv_r$  is shown as a function of pressure in fig. 12; almost the entire moisture transport is directed inward. Table 8 gives the results in units of 10<sup>12</sup> kilowatt-hours per day, which is equivalent to 10<sup>13</sup> cal/sec or  $3.6 \times 10^{25}$  ergs/day.

As would be expected from fig. 10, balance is very nearly obtained. In the inner part of the cyclone, both latent and sensible heat are converted to potential energy as the mass rises, and this potential energy is exported to other circulations. The latent heat inflow can be converted to precipitation depth, which can serve as an order-of-magnitude check on the validity of the moisture-flow calculation. Inside the 2-deg radius, the mean precipitation computed from table 8 is 10 cm/day, a reasonable value which agrees well with the computation of Hughes (1952).

The efficiency ( $E$ ) of a thermal engine in converting heat to mechanical energy can be defined as the ratio of the mechanical energy produced to the heat released. From table 6, the kinetic energy produced and dissipated is  $150 \times 10^{18}$  ergs/sec or  $0.36 \times 10^{12}$  kilowatt-hours per day. Thus,  $E = 3$  per cent, a somewhat higher value than is usually estimated for the general circulation and for other types of disturbances. In terms of energy production by man, the fraction of latent heat released which is converted to kinetic energy is very large. The electric power production of the United States is about  $2 \times 10^9$  kilowatt-hours per day; hence, the mechanical energy generation in hurricanes is 200 times as large. The energy of the microstructure within hurricanes may be assessed as at least 1 to 2 per cent of that of the mean circulation. Since, as shown by Palmén and Jordan (1955), kinetic energy and energy dissipation or production per day are roughly equal, we can say that the kinetic-energy producing fraction of the heat release in the microstructure has at least the order of magnitude of the electric power production of the United States. As is well known, the symmetrical part of the circulation of hurricanes is essentially stable with respect to disrupting influence of the microstructure.

We can finally ask whether hurricanes are energy exporting circulations. For this purpose, we divide the enthalpy into internal energy and the work done by pressure forces. Thus,  $c_p T = c_v T + p/\rho$ . Inserting

TABLE 9. Calculation of energy export from hurricanes (10<sup>12</sup> kilowatt-hours per day).

Term	Value	
Gain of real heat	13.3	
Work done by pressure forces	7.7	
Export of potential energy		36.4
Import of internal energy		-15.1
Balance	21.0	21.3

in (24) and expressing the gain of heat as a volume integral, we have

$$\int_V \rho \frac{dh}{dt} dV + \int_0^{2\pi} \int_0^{H_t} p v_r dz r d\theta = - \frac{1}{g} \int_0^{2\pi} \int_{p=100}^{p_0} (\Phi + c_v T) v_r dp r d\theta, \quad (25)$$

where  $H_t$  is the height of the top of the storm. In this equation, the net transport of potential and internal energy appears explicitly, as does the work of the pressure forces across the cylinder over which the integration extends. Table 9 shows the balance. We find that a strong net outflow of potential plus internal energy takes place. This energy, produced by transformations within the core, is available to drive other portions of the general circulation.

REFERENCES

Byers, H. R., 1944: *General meteorology*. New York, McGraw-Hill Book Co., 645 pp.  
 Ekman, V. W., 1905: On the influence of the earth's rotation on ocean currents. *Ark. Mat. Astr. Fys.*, 2, No. 11, 52 pp.  
 Haurwitz, B., 1935: The height of tropical cyclones and of the 'eye' of the storm. *Mon. Wea. Rev.*, 63, 45-49.  
 Hughes, L. A., 1952: On the low-level wind structure of tropical storms. *J. Meteor.*, 9, 422-428.  
 Jordan, E. S., 1952: An observational study of the upper wind circulation around tropical storms. *J. Meteor.*, 9, 340-346.  
 Kleinschmidt, E., 1951: Grundlagen einer Theorie der tropischen Zyklonen. *Archiv Meteor. Geophys. Bioklim.*, A, 4, 53-72.  
 Palmén, E., and C. L. Jordan, 1955: Note on the release of kinetic energy in tropical cyclones. *Tellus*, 7, 186-189.  
 Palmén, E., and L. Laurila, 1938: Ueber die Einwirkung eines Sturmes auf den hydrographischen Zustand im noerdlichen Ostseegebiet. *Soc. Sci. Fen., Com. Phys.-Math.*, 10, No. 1, 53 pp.  
 Pfeffer, R. L., 1956: *Concerning the mechanics of hurricanes*. [Sci. Rep. 4, Contract AF19(604)-1000], Cambridge, Mass. Inst. Tech.  
 Riehl, H., 1954: *Tropical meteorology*. New York, McGraw-Hill Book Co., 392 pp.  
 —, et al, 1951: The northeast trade of the Pacific ocean. *Quart. J. r. meteor. Soc.*, 77, 598-627.  
 Schacht, E. J., 1946: A mean hurricane sounding for the Caribbean area. *Bull. Amer. meteor. Soc.*, 27, 324-327.  
 Sheppard, P. A., and H. M. Omar, 1952: The wind stress over the ocean from observations in the trades. *Quart. J. r. meteor. Soc.*, 78, 583-590.